Reduction-Oxidation Properties of Organo-transition Metal Complexes. Part 33.[1] Ligand- *vs.* Metal-based Oxidation of Cyano-bridged Catecholatoruthenium–Manganese Carbonyl Compounds: The X-Ray Crystal Structure of *cis*-[(dppe)(Et$_3$P)(OC)$_2$Mn(μ-CN)Ru(CO)$_2$(PPh$_3$)(*o*-O$_2$C$_6$Cl$_4$)]·CH$_2$Cl$_2$ *

Aristides Christofides, Neil G. Connelly, Holly J. Lawson, Andrew C. Loyns, A. Guy Orpen, Mark O. Simmonds and Gillian H. Worth
School of Chemistry, University of Bristol, Bristol BS8 1TS, UK

The reactions of *cis*- or *trans*-[Mn(CN)(CO)$_2${P(OPh)$_3$}(dppm)] (dppm = Ph$_2$PCH$_2$PPh$_2$) or *cis*-[Mn(CN)(CO)$_2$(PEt$_3$)(dppe)] (dppe = Ph$_2$PCH$_2$CH$_2$PPh$_2$) with [{Ru(CO)$_2$(PPh$_3$)(μ-*o*-O$_2$C$_6$Cl$_4$)}$_2$] give the heterobinuclear complexes *cis*- and *trans*-[(dppm){(PhO)$_3$P}(OC)$_2$Mn(μ-CN)Ru(CO)$_2$(PPh$_3$)(*o*-O$_2$C$_6$Cl$_4$)] **5** and **6** and *cis*-[(dppe)(Et$_3$P)(OC)$_2$Mn(μ-CN)Ru(CO)$_2$(PPh$_3$)(*o*-O$_2$C$_6$Cl$_4$)] **7**. The X-ray crystal structure of **7** shows approximately octahedrally co-ordinated ruthenium and manganese centres linked by a μ-CN ligand C-bonded to Mn and N-bonded to Ru, the Ru–N–C–Mn system is slightly non-linear, with angles at C and N of 174.8(5) and 171.4(4)°, despite the formal sp hybridisation at these atoms. Complexes **5**–**7** undergo two sequential one-electron oxidations at a platinum electrode in CH$_2$Cl$_2$. Treatment with 1 equivalent of [NO][PF$_6$] gives the monocations *cis*- and *trans*-[(dppm){(PhO)$_3$P}(OC)$_2$Mn(μ-CN)Ru(CO)$_2$(PPh$_3$)(*o*-O$_2$C$_6$Cl$_4$)]$^+$ **5**$^+$ and **6**$^+$ and *cis*-[(dppe)(Et$_3$P)(OC)$_2$Mn(μ-CN)Ru(CO)$_2$(PPh$_3$)(*o*-O$_2$C$_6$Cl$_4$)]$^+$ **7**$^+$ the voltammetry and IR and ESR spectra of which show electron removal from the catecholate ligand. The reaction of [{Ru(CO)$_2$(PPh$_3$)(μ-*o*-O$_2$C$_6$Cl$_4$)}$_2$] with *trans*-[Mn(CN)(CO)$_2${P(OPh)$_3$}(dppm)]$^+$ also gave **6**$^+$ but the analogous reaction with *trans*-[Mn(CN)(CO)$_2$(PEt$_3$)(dppe)]$^+$ gave **7**$^+$. In both cases, intramolecular electron transfer from the O,O-chelate to Mn$^{\text{II}}$ follows cyanide-bridge formation; in the second case this is accompanied by *trans*–*cis* isomerisation at the resulting manganese(I) centre. Subsequent oxidation of **5**$^+$–**7**$^+$ occurs at the manganese(II) centre and is accompanied by *cis*–*trans* isomerisation. The reaction of the more electron-rich manganese(I) donor *trans*-[Mn(CN)(CO)(dppm)$_2$] with [{Ru(CO)$_2$(PPh$_3$)(μ-*o*-O$_2$C$_6$Cl$_4$)}$_2$] gives *trans*-[(dppm)$_2$(OC)Mn(μ-CN)Ru(CO)$_2$(PPh$_3$)(*o*-O$_2$C$_6$Cl$_4$)] **8** which also undergoes two one-electron oxidations. In this case, however, oxidation at Mn$^{\text{I}}$ precedes that at the catecholate ligand; the manganese(II)-containing monocation **8**$^+$ is synthesised from **8** and [N$_2$C$_6$H$_4$F-*p*]$^+$ or directly from [{Ru(CO)$_2$(PPh$_3$)(μ-*o*-O$_2$C$_6$Cl$_4$)}$_2$] and *trans*-[Mn(CN)(CO)(dppm)$_2$]$^+$. Changes in ν(CN)$_{\text{bridge}}$ appear to be diagnostic of oxidation at the C- or N-bonded centre of the binuclear complexes.

The nitrogen atom of the cyanide ligand of electron-rich manganese carbonyl derivatives is nucleophilic and may be protonated, as in [Mn(CNH)(CO)$_2${P(OPh)$_3$}(dppm)]$^{2+}$ (dppm = Ph$_2$PCH$_2$PPh$_2$),[2] methylated by MeI to give *cis*- or *trans*-[Mn(CNMe)(CO)$_2${P(OPh)$_3$}(dppm)]$^+$,[3] or undergo allylic alkylation with [Fe{P(OMe)$_3$}(NO)$_2$(η-C$_3$H$_4$R)]$^+$ to yield *trans*-[Mn(CNCH$_2$CRCH$_2$)(CO)(dppm)$_2$]$^+$ (R = H or Me).[4] It may also bind to a second metal atom so that replacement of the metal-bound bromide of *cis*- or *trans*-[MnBr(CO)$_2${P(OPh)$_3$}(dppm)] by *cis*- or *trans*-[Mn(CN)(CO)$_2${P(OPh)$_3$}(dppm)] (in the presence of Tl$^+$) provides a route to the complexes **1**$^+$–**4**$^+$. In these species *cis*–*trans* isomerisation, induced by one-electron oxidation, provides[5] a probe of the intermetallic interaction in the mixed-valence dications **1**$^{2+}$–**4**$^{2+}$. We have also recently noted[6] the use of *cis*- and *trans*-[Mn(CN)(CO)$_2$L(L–L)], *trans*-[Mn(CN)(CO)$_2$L(L–L)]$^+$ [L = PEt$_3$, L–L = dppe; L = P(OPh)$_3$, L–L = dppm], and *trans*-[Mn(CN)(CO)(dppm)$_2$]^z (z = 0 and 1) in the synthesis of cyanide-bridged heterobinuclear complexes and we now give details of species where the metal-based Mn$^{\text{I}}$–Mn$^{\text{II}}$ couple is linked to a ruthenium(II) catecholate/*o*-benzosemiquinone centre. Not only does the oxidative isomerisation process at manganese reflect the interaction between metal- and ligand-based redox centres but the alteration of the ancillary ligands on manganese provides a means by which the site of oxidation may be systematically changed.

Results and Discussion

The addition of *cis*- or *trans*-[Mn(CN)(CO)$_2${P(OPh)$_3$}(dppm)] or *cis*-[Mn(CN)(CO)$_2$(PEt$_3$)(dppe)] (dppe = Ph$_2$PCH$_2$CH$_2$PPh$_2$) to [{Ru(CO)$_2$(PPh$_3$)(μ-*o*-O$_2$C$_6$Cl$_4$)}$_2$] (Fig. 1) in CH$_2$Cl$_2$ immediately gave orange solutions from which good yields of the heterobinuclear complexes *cis*-[(dppm){(PhO)$_3$P}(OC)$_2$Mn(μ-CN)Ru(CO)$_2$(PPh$_3$)(*o*-O$_2$C$_6$Cl$_4$)] **5**, *trans*-[(dppm){(PhO)$_3$P}(OC)$_2$Mn(μ-CN)Ru(CO)$_2$(PPh$_3$)(*o*-O$_2$C$_6$Cl$_4$)] **6** and *cis*-[(dppe)(Et$_3$P)(OC)$_2$Mn(μ-CN)Ru(CO)$_2$(PPh$_3$)(*o*-O$_2$C$_6$Cl$_4$)] **7** were readily isolated as air-stable, yellow or orange solids (Table 1). In each case the geometries of the individual metal dicarbonyl units may be simply deduced from the IR carbonyl spectra; the two bands associated with the *cis*-Ru(CO)$_2$ group are essentially inde-

---

* [1,2-Bis(diphenylphosphino)ethane-1$\kappa P,P'$]tetracarbonyl-1$\kappa^2 C$,2$\kappa^2 C$-μ-cyano-1:2$\kappa^2 C$:N-tetrachloro-*o*-catecholato-2$\kappa^2 O,O'$-triethylphosphine-1κP-triphenylphosphine-2κP-manganeseruthenium–dichloromethane (1/1).

Supplementary data available: see Instructions for Authors, *J. Chem. Soc., Dalton Trans.*, 1991, Issue 1, pp. xviii–xxii.

Table 1 Analytical and IR spectroscopic data for $[L_xMn(\mu\text{-CN})Ru(CO)_2(PPh_3)(o\text{-}O_2C_6Cl_4)]^z$

			Analysis (%)[b]			IR[c]/cm^{-1}		
L_x	Z[a]	Colour	C	H	N	ν(CN)[d]	ν(CO)(Ru)	ν(CO)(Mn)
cis-$(CO)_2\{P(OPh)_3\}$(dppm)	0	Orange	57.3 (57.8)	3.6 (3.5)	0.9 (0.9)	2132	2051, 1983	1971(sh), 1919
trans-$(CO)_2\{P(OPh)_3\}$(dppm)	0	Yellow	57.3 (57.8)	3.9 (3.5)	0.8 (0.9)	2120	2048, 1982	1938
cis-$(CO)_2(PEt_3)$(dppe)	0	Orange	56.0 (55.5)	4.5 (4.1)	1.2 (1.1)	2118	2049, 1983	1943, 1883
cis-$(CO)_2\{P(OPh)_3\}$(dppm)	1	Dark red	52.3 (52.7)	3.4 (3.2)	0.7 (0.9)	2120	2081, 2027	1977, 1927
trans-$(CO)_2\{P(OPh)_3\}$(dppm)	1	Red-brown	52.7 (52.7)	3.4 (3.2)	0.8 (0.9)	2105	2080, 2025	1939
cis-$(CO)_2(PEt_3)$(dppe)	1	Dark red	50.0 (50.0)	4.0 (3.7)	1.2 (1.0)	2106	2080, 2026	1949, 1895
trans-(CO)$(dppm)_2$	0	Orange	61.1 (60.7)	4.2 (3.9)	0.9 (0.9)	2095	2050, 1983	1871
trans-(CO)$(dppm)_2$	1	Orange-red	55.1 (55.5)	4.1 (3.5)	0.8 (0.8)	2126	2050, 1983	1947m

[a] Cationic complexes analysed as $[PF_6]^-$ salts. [b] Calculated values in parentheses. [c] In CH_2Cl_2. Strong absorptions unless stated otherwise; sh = shoulder, m = medium. [d] Medium weak.

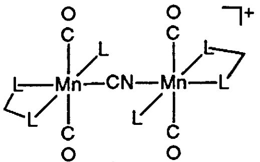

1⁺

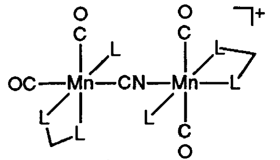

2⁺

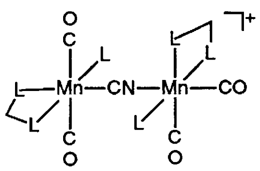

3⁺

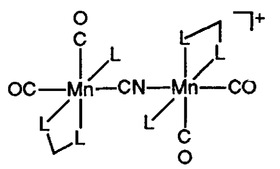

4⁺

L - L = dppm, L = P(OPh)3

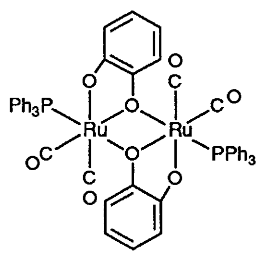

Fig. 1 The proposed[11] structure of $[\{Ru(CO)_2(PPh_3)(\mu\text{-}o\text{-}O_2C_6Cl_4)\}_2]$; chlorine atoms on the rings are omitted for clarity

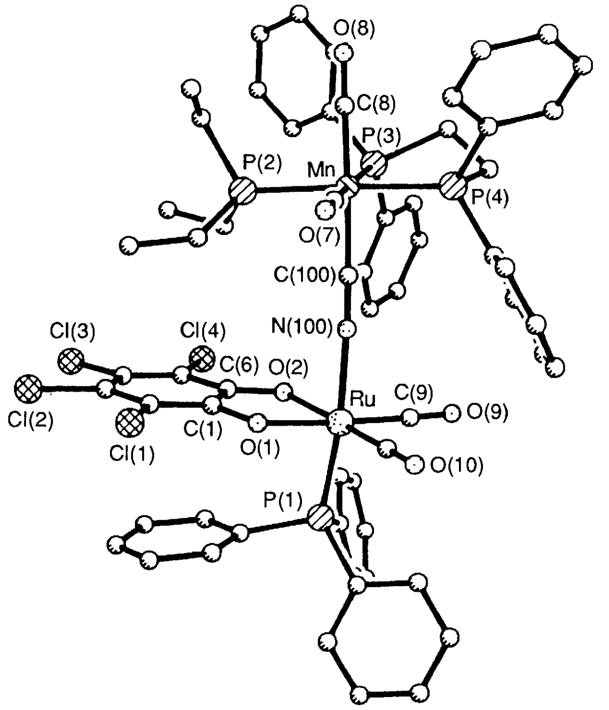

Fig. 2 The molecular structure of compound 7 showing the atom labelling scheme

pendent of the nature of the ligands on the manganese centre whereas those of the $Mn(CO)_2$ moiety vary with both the geometry of the complex (two bands for the *cis* isomers **5** and **7**, one for the *trans* isomer **6**) and the nature of the bonded P-donors. On bridge formation the cyanide absorption increases in intensity, presumably as a consequence of the increase in the polarity of the CN bond. The ν(CN) band is also shifted to higher energy, as previously found[7,8] for other μ-CN complexes and explained[9] in terms of increased electron withdrawal from the lowest filled CN σ*(s) orbital on N-co-ordination.

Although the arrangement of each dicarbonyl unit, and the bridging nature of the cyanide ligand, were readily established by IR spectroscopy, the overall structure of the binuclear species could not be assigned unambiguously. The structure of complex **7** (Fig. 2), as its dichloromethane solvate, was therefore determined by a room-temperature single-crystal X-ray diffraction study; selected bond lengths and angles are given in Table 2. Compound **7** consists of approximately octahedrally co-ordinated ruthenium and manganese centres linked by a μ-CN ligand C-bonded to Mn and N-bonded to Ru. The co-ordination sphere at Ru is completed by a PPh_3 ligand *trans* to the cyanide bridge, two *cis* CO ligands and a chelating o-$O_2C_6Cl_4$ ligand bonded through its oxygen atoms. At Mn the ligand *trans* to the μ-CN group is a carbonyl, there is a second CO *cis* to these ligands and *trans* to one of the phosphorus atoms of a chelating dppe ligand, and the co-ordination sphere at Mn is completed by a PEt_3 ligand *trans* to the other dppe phosphorus. Distortions from ideal octahedral angles in the co-ordination spheres of the metals are largely associated with the restrictions imposed by the chelating ligands [O(1)–Ru–O(2) 80.9(1), P(3)–Mn–P(4) 83.8(1)°]. The dimensions of the o-$O_2C_6Cl_4$ ligand are consistent with it being in the catecholate, dianionic, form with all the C–C distances close to 1.4 Å and C–O *ca.* 1.33 Å {*cf.* similar values in the mononuclear catecholate $[Ru(CO)_2(PPh_3)_2(o\text{-}O_2C_6Cl_4)]$, but more varied C–C and shorter C–O distances in the semiquinone complex cation $[Ru(CO)_2(PPh_3)_2(o\text{-}O_2C_6Cl_4)]^+$ *i.e.* C–O *ca.* 1.29, (O)C–C(O) 1.44 Å}[10]. The variation in the Mn–P distances is consistent with the effects of the substituents at the phosphorus and of the *trans* ligand. Thus the Mn–P bond *trans* to CO [Mn–P(3) 2.360(2) Å] is the longest, that for phosphorus with phenyl substituents *trans* to a phosphine is the shortest [Mn–P(4) 2.289(2) Å], and

Table 2 Intramolecular bond distances (Å) and angles (°) for compound **7**·CH_2Cl_2

Ru–P(1)	2.363(2)	Ru–O(1)	2.068(4)	P(1)–C(20)	1.821(8)	P(1)–C(90)	1.839(6)
Ru–O(2)	2.071(4)	Ru–C(9)	1.872(7)	P(1)–C(110)	1.832(6)	P(3)–C(30)	1.826(6)
Ru–C(10)	1.885(6)	Ru–N(100)	2.101(5)	Cl(1)–C(2)	1.718(6)	Cl(2)–C(3)	1.731(9)
Mn–P(3)	2.360(2)	Mn–P(2)	2.323(2)	Cl(3)–C(4)	1.743(8)	Cl(4)–C(5)	1.734(6)
Mn–P(4)	2.289(2)	Mn–C(7)	1.797(6)	C(100)–N(100)	1.167(8)	C(80)–C(81)	1.514(12)
Mn–C(8)	1.790(7)	Mn–C(100)	1.982(6)	C(1)–C(6)	1.410(8)	C(1)–C(2)	1.410(10)
O(9)–C(9)	1.141(9)	O(10)–C(10)	1.127(7)	C(2)–C(3)	1.393(10)	C(3)–C(4)	1.378(10)
O(1)–C(1)	1.318(7)	O(2)–C(6)	1.334(8)	C(4)–C(5)	1.393(11)	C(5)–C(6)	1.407(9)
P(1)–Ru–O(1)	91.1(1)	P(1)–Ru–O(2)	86.1(1)	P(4)–Mn–C(7)	90.6(2)	P(3)–Mn–C(8)	86.0(2)
O(1)–Ru–O(2)	80.9(1)	P(1)–Ru–C(9)	91.2(2)	P(3)–Mn–C(7)	173.6(3)	P(2)–Mn–C(7)	90.8(2)
O(1)–Ru–C(9)	176.4(2)	O(2)–Ru–C(9)	96.5(2)	P(4)–Mn–C(8)	91.7(2)	P(2)–Mn–C(8)	91.7(2)
P(1)–Ru–C(10)	95.9(2)	O(1)–Ru–C(10)	92.4(2)	C(7)–Mn–C(8)	90.9(3)	P(3)–Mn–C(100)	97.4(2)
O(2)–Ru–C(10)	173.0(2)	C(9)–Ru–C(10)	90.1(3)	P(2)–Mn–C(100)	87.0(2)	P(4)–Mn–C(100)	90.7(2)
P(1)–Ru–N(100)	170.9(1)	O(1)–Ru–N(100)	85.6(2)	C(7)–Mn–C(100)	85.8(3)	C(8)–Mn–C(100)	176.4(3)
O(2)–Ru–N(100)	85.0(2)	C(9)–Ru–N(100)	91.8(3)	Ru–P(1)–C(20)	109.6(2)	Ru–P(1)–C(90)	114.0(2)
C(10)–Ru–N(100)	92.7(2)	P(3)–Mn–P(2)	94.9(1)	Mn–P(3)–C(30)	118.6(2)	Mn–P(3)–C(40)	124.4(2)
P(3)–Mn–P(4)	83.8(1)	P(2)–Mn–P(4)	177.2(1)	Mn–C(100)–N(100)	174.8(5)	Ru–N(100)–C(100)	171.4(4)

that of the trialkylphosphine is intermediate in length [Mn–P(2) 2.323(2) Å].

The Ru–N, C–N and Mn–CN distances [2.101(5), 1.167(8), 1.982(6) Å] are similar, albeit more precisely determined, to those in homodinuclear μ-CN species {*e.g.* Ru–N and N–C, 2.07(1) and 1.14(2) Å in $[(\eta\text{-}C_5H_5)(dppe)Ru(\mu\text{-}CN)Ru(\eta\text{-}C_5H_5)(PPh_3)_2]^+$;[8] Mn–C and C–N, 2.004(11) and 1.107(15) Å in $[\{fac\text{-}Mn(CO)_3(phen)\}_2(\mu\text{-}CN)]^+$ (phen = 1,10-phenanthroline)}[3]. As in these μ-CN species, the angles at CN, although indicative of sp hybridisation at these atoms, are apparently quite easily deformed from linearity. In **7** the angles at C and N are 174.8(5) and 171.4(4)°, *cf.* 175(1) and 168(1)° in the diruthenium species[8] and 168.2(10) and 171.2(10)° in the dimanganese complex.[3]

The cyclic voltammograms of compounds **5** and **7** show two oxidation waves in the potential range 0.0–1.8 V; that of **7** is shown in Fig. 3 and the potential data for both complexes are given in Table 3. In each case, the first wave is fully reversible $[(i_p)_{ox}/(i_p)_{red} = 1.0$ for scan rates, v, between 50 and 500 mV $s^{-1}]$ and diffusion controlled $[(i_p)_{ox}/v^{\frac{1}{2}} = \text{constant}]$ with the potential essentially independent of the nature of the manganese centre but very similar to that found[11] for the one-electron oxidation of $[Ru(CO)_2(PPh_3)_2(o\text{-}O_2C_6Cl_4)]$. By contrast, the second wave is chemically irreversible, with the peak potential dependent on the ligands on manganese and with an associated product wave at a potential more negative by *ca* 0.4–0.5 V. These results strongly suggest that the initial oxidation step occurs at the ruthenium-bound catecholate ligand and that the second, manganese-centred oxidation, results in isomerisation to give *trans*-$[(L\text{-}L)L(OC)_2Mn(\mu\text{-}CN)Ru(CO)_2(PPh_3)(o\text{-}O_2C_6Cl_4)]^{2+}$ as the final product. The identity of this final product is supported by the cyctic voltammogram of **6** which shows two reversible oxidation waves, the second at a potential identical to that of the product wave of **5**; the first wave again appears at a very similar potential to that of the first oxidation of $[Ru(CO)_2(PPh_3)_2(o\text{-}O_2C_6Cl_4)]$.[11] It is also noteworthy that N-co-ordination leads to a substantial shift to more positive potentials of the waves associated with the manganese(I) oxidative isomerisation process. Compare, for example, complex **5** (0.96 and 1.51 V) with *cis*-$[Mn(CN)(CO)_2\{P(OPh)_3\}(dppm)]$ (0.64 and 1.16 V).[2] Clearly, such co-ordination results in reduced electron density on manganese as is also suggested by comparing ν(CO) for the *cis*-$Mn(CO)_2$ groups of **5** (1971 and 1919 cm^{-1}) and *cis*-$[Mn(CN)(CO)_2\{P(OPh)_3\}(dppm)]$ (1969 and 1910 cm^{-1}).[3]

The proposal of catecholate-centred oxidation for compounds **5**–**7** was readily confirmed by the isolation and spectroscopic characterisation of the monocations $\mathbf{5}^+$–$\mathbf{7}^+$; the addition of a stoichiometric (1:1) quantity of $[NO][PF_6]$ to **5** or **7** in CH_2Cl_2 rapidly gave a dark red solution from which moderate yields of the red-brown $[PF_6]^-$ salts were isolated. The products were characterised by elemental analysis, voltammetry (both cyclic and rotating platinum electrode voltammograms were identical to those of the neutral precursors except that the wave at *ca.* 0.5 V was a reduction wave) and by IR and ESR spectroscopy. Both $\mathbf{5}^+$ and $\mathbf{7}^+$ show four carbonyl absorptions, confirming the retention of geometry at both metal centres. The two bands associated with the ruthenium centre are shifted to higher energy by *ca.* 30–40 cm^{-1} similar to the changes observed[11] when $[Ru(CO)_2(PPh_3)_2(o\text{-}O_2C_6Cl_4)]$ was oxidised to $[Ru(CO)_2(PPh_3)_2(o\text{-}O_2C_6Cl_4)]^+$; the small increases in ν(CO) for the manganese-bound carbonyls (*ca.* 6–10 cm^{-1}) also suggest that the oxidation is largely localised on the catecholate ligand.

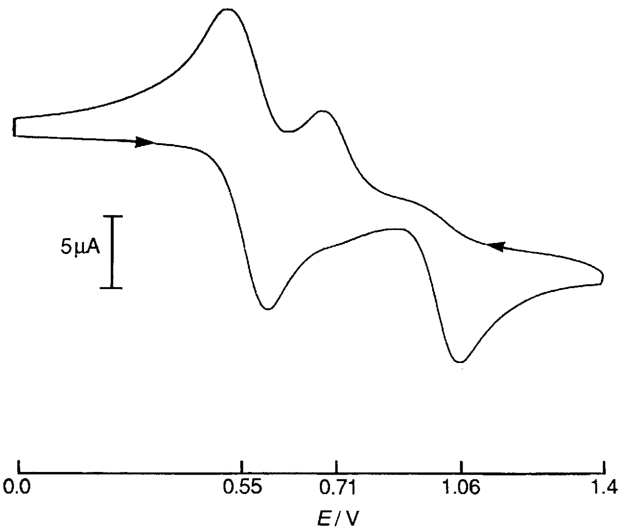

Fig. 3 Cyclic voltammogram of *cis*-$[(dppe)(Et_3P)(OC)_2Mn(\mu\text{-}CN)Ru(CO)_2(PPh_3)(o\text{-}O_2C_6Cl_4)]$ from 0.0 to 1.4 V

The room-temperature ESR spectra of $\mathbf{5}^+$ and $\mathbf{7}^+$ confirm the nature of the half-occupied orbital in showing a doublet $[A(^{31}P)$ 8.3 G $(8.3 \times 10^{-4}$ T)] with $g_{av} = 2.004$, close to the free-electron value. A similar spectrum (but with coupling to both axial phosphorus atoms) was observed[11] for $[Ru(CO)_2(PPh_3)_2(o\text{-}O_2C_6Cl_4)]^+$ which has[10] a semiquinone ligand bonded to the ruthenium centre.

Complex $\mathbf{7}^+$ can also be prepared by the direct addition of the paramagnetic cyanomanganese(II) ligand *trans*-$[Mn(CN)(CO)_2(PEt_3)(dppe)]^+$ to $[\{Ru(CO)_2(PPh_3)(\mu\text{-}o\text{-}O_2C_6Cl_4)\}_2]$. The most likely mechanism for this reaction involves initial co-ordination of the $Mn^{II}(CN)$ group to ruthenium followed by

Table 3 Cyclic voltammetric data[a] for $[L_xMn(\mu\text{-}CN)Ru(CO)_2(PPh_3)(o\text{-}O_2C_6Cl_4)]^z$

L_x	Z	Potential[b]/V E(Ru)[c]	 E(Mn)[d]
cis-$(CO)_2\{P(OPh)_3\}$(dppm)	0	0.52	1.51(I), (0.96)
trans-$(CO)_2\{P(OPh)_3\}$(dppm)	0	0.51	1.03
cis-$(CO)_2(PEt_3)$(dppe)	0	0.55	1.06(I) (0.71)
cis-$(CO)_2\{P(OPh)_3\}$(dppm)	1	0.51	1.46(I) (0.98)
trans-$(CO)_2\{P(OPh)_3\}$(dppm)	1	0.51	1.03
cis-$(CO)_2(PEt_3)$(dppe)	1	0.55	1.13(I) (0.72)
trans-(CO)$(dppm)_2$	0	0.62	0.17
trans-(CO)$(dppm)_2$	1	0.62	0.16

[a] In CH_2Cl_2 at a platinum-bead electrode. Under the conditions used the potentials for the couples $[Fe(\eta\text{-}C_5H_5)_2]^+$–$[Fe(\eta\text{-}C_5H_5)_2]$ and $[Fe(\eta\text{-}C_5Me_5)_2]^+$–$[Fe(\eta\text{-}C_5Me_5)_2]$ are 0.47 and −0.09 V respectively. [b] E° for reversible wave unless otherwise stated. The oxidation peak potential, $(E_p)_{ox}$, at a scan rate of 200 mV s^{-1} is given for an irreversible (I) wave; numbers in parentheses are $(E_p)_{red}$, at a scan rate of 200 mV s^{-1}, for the reversible product wave. [c] Oxidation at the ruthenium catecholate centre. [d] Oxidation at the manganese(I) centre.

intramolecular electron transfer to give Mn^I and the semiquinone ligand of the product. Such a mechanism depends on the ability of the cyanide ligand to act as a conducting bridge (even though the cyclic voltammograms of **5**–**7** suggest little or no communication between the two redox centres). There is, of course, ample evidence for intramolecular electron transfer *via* cyanide bridges, in Prussian Blue and more recently in $[(NC)_5Fe(\mu\text{-}NC)Fe(CN)_4(NH_3)]^{4-}$ where there is antiferromagnetic coupling between the two iron centres.[12] An alternative mechanism for the formation of $\mathbf{7}^+$ namely oxidation of $[\{Ru(CO)_2(PPh_3)(\mu\text{-}o\text{-}O_2C_6Cl_4)\}_2]$ by Mn^{II} followed by reaction of the resulting manganese(I) complex with a binuclear cation such as $[\{Ru(CO)_2(PPh_3)(\mu\text{-}o\text{-}O_2C_6Cl_4)\}_2]^{z+}$ (z = 1 or 2) is unlikely; the cyclic voltammogram of $[\{Ru(CO)_2(PPh_3)(\mu\text{-}o\text{-}O_2C_6Cl_4)\}_2]$ shows only an irreversible oxidation wave at *ca.* 1.0 V, *i.e.* at a potential rather more positive than that at which *trans*-$[Mn(CN)(CO)_2(PEt_3)(dppe)]^+$ is reduced (*ca.* 0.36 V).

The intramolecular electron-transfer step is followed by *trans–cis* isomerisation of the ruthenium-bound *trans*-$[Mn(CN)(CO)_2(PEt_3)(dppe)]$ unit to give $\mathbf{7}^+$ as the final product; rapid isomerisation similarly occurs[2] on reduction of the uncoordinated, mononuclear cyano-complex. By contrast, *trans*-$[Mn(CN)(CO)_2\{P(OPh)_3\}(dppm)]$ is thermally stable so that the reaction of *trans*-$[Mn(CN)(CO)_2\{P(OPh)_3\}(dppm)]^+$ with $[\{Ru(CO)_2(PPh_3)(\mu\text{-}o\text{-}O_2C_6Cl_4)\}_2]$ gives $\mathbf{6}^+$ an isomer of $\mathbf{5}^+$. Here again, the IR and ESR spectra and the cyclic voltammetry are consistent with a semiquinone/manganese(I) complex but the geometry at the latter site is retained following the intramolecular electron-transfer reaction. The changes in ν(CN) when compounds **5**–**7** undergo one-electron oxidation are notable in that there is a *decrease* in energy by 12–15 cm^{-1}. Where the redox activity of cyanide-bridged complexes has been previously studied[13] little or no data have been reported concerning $\nu(CN)_{bridge}$. In the case of the iron-(II) and -(III) complexes $[(NC)_5Fe(\mu\text{-}CN)Co^{III}(CN)_5]^z$ (z = 6 or 5 respectively) an increase in energy of $\nu(CN)_{bridge}$ was noted[14] 'as expected'. An increase in ν(CN) is certainly expected when a mononuclear cyanide complex undergoes one-electron oxidation because of decreased d_π-back bonding to the p_{π^*}(CN) orbital (*cf.* metal carbonyl complexes). It is also reasonable to expect a similar change in $\nu(CN)_{bridge}$ when the C-bonded terminus is oxidised. It is unclear, however, why the decrease in $\nu(CN)_{bridge}$ is observed on oxidation of the N-bound ruthenium groups of **5**–**7**. Whatever the reason, however, the observation of a dependence on oxidation site of the shift in $\nu(CN)_{bridge}$ may have diagnostic value, as noted below.

We have been unable to isolate the products of the second oxidations of **5**–**7**, prolonged contact between the neutral heterobinuclear complexes and $[NO][PF_6]$ apparently ultimately leading to cleavage of the cyanide bridge. However, the IR spectrum shown in Fig. 4(*c*), observed soon after adding 2 equivalents of $[NO][PF_6]$ to **7** [Fig. 4(*a*)], or of 1 equivalent to $\mathbf{7}^+$ [Fig. 4(*b*)], can be assigned to the short-lived dication *trans*-$[(dppe)(Et_3P)(OC)_2Mn(\mu\text{-}CN)Ru(CO)_2(PPh_3)(o\text{-}O_2C_6Cl_4)]^{2+}$, *i.e.* the product expected on the basis of the cyclic voltammetry (CV) study described above. The red-purple solution formed shows three carbonyl bands at 2088, 2032 and 1980 cm^{-1} the last of which may be assigned to a *trans*-$Mn^{II}(CO)_2$ unit by comparison with that of *trans*-$[Mn(CN)(CO)_2(PEt_3)(dppe)]^+$ [ν(CO) 1971 cm^{-1}]; the bands at higher wavenumber may be assigned to the *cis*-$Ru(CO)_2$ group, shifted to higher energy by only *ca.* 7–8 cm^{-1} (*cf.* $\mathbf{7}^+$). Support for C-bonded manganese(I) as the site of the second oxidation step is also provided by the shift of $\nu(CN)_{bridge}$ to higher energy (from 2106 cm^{-1} for $\mathbf{7}^+$ to 2132 cm^{-1}). Unfortunately, no satisfactory ESR spectrum could be recorded and the magnetic properties of the proposed dication remain unresolved.

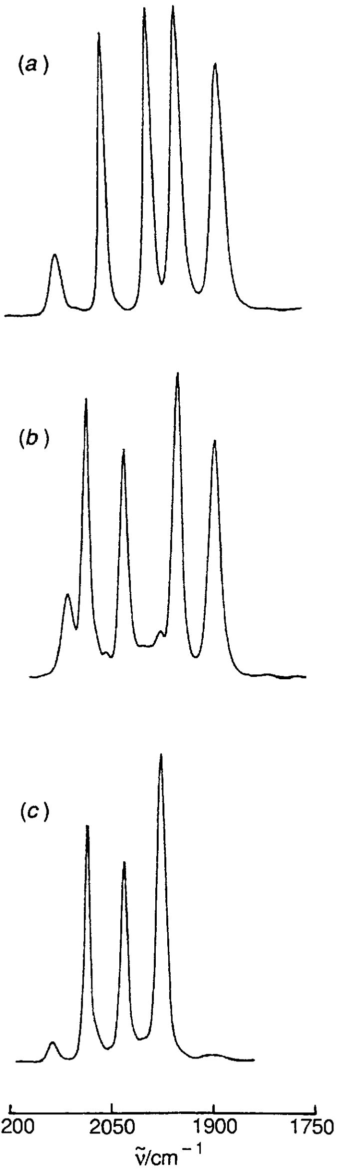

Fig. 4 The IR spectra of (*a*) compound **7**, (*b*) $\mathbf{7}^+$ and (*c*) *trans*-$[(dppe)(Et_3P)(OC)_2Mn(\mu\text{-}CN)Ru(CO)_2(PPh_3)(o\text{-}O_2C_6Cl_4)]^{2+}$

On adding *trans*-$[Mn(CN)(CO)(dppm)_2]$ to $[\{Ru(CO)_2(PPh_3)(\mu\text{-}o\text{-}O_2C_6Cl_4)\}_2]$ the orange complex *trans*-$[(dppm)_2(OC)Mn(\mu\text{-}CN)Ru(CO)_2(PPh_3)(o\text{-}O_2C_6Cl_4)]$ **8** was readily isolated. The cyclic voltammogram of this species (Table 3) also shows two oxidation waves but in this case both are fully reversible. Moreover, and in sharp contrast to **5**–**7**, the use of the more electron-rich cyanomanganese(I) donor results in manganese-based oxidation as the first process. Thus, the chemical oxidation of **8** with 1 equivalent of $[N_2C_6H_4F\text{-}p][PF_6]$ gave $\mathbf{8}^+$ as an air-stable orange-red solid (which may also be prepared, more conveniently, by the direct addition of *trans*-$[Mn(CN)(CO)(dppm)_2]^+$ to $[\{Ru(CO)_2(PPh_3)(\mu\text{-}o\text{-}O_2C_6Cl_4\}_2])$. The IR spectrum of $\mathbf{8}^+$ shows that the band associated with the Mn(CO) group is shifted to higher energy on oxidation, by 76 cm^{-1}, a shift very similar to that observed (77 cm^{-1}) for the oxidation of *trans*-$[Mn(CN)(CO)(dppm)_2]$ to its monocation. By contrast, no difference is observed in the two bands associated with the $Ru(CO)_2$ group. The cyanide stretch of compound **8** is increased in energy (by 31 cm^{-1}) also suggesting oxidation at the C-bound centre. Furthermore, the ESR spectrum [tetrahydrofuron (thf)–CH_2Cl_2 glass, at 77 K] closely resembles that of *trans*-$[Mn(CN)(CO)(dppm)_2]^+$.[15] The addition of a second equivalent of one-electron oxidant to **8** in CH_2Cl_2 led to irreversible changes in the cyclic voltammogram, and to IR carbonyl absorptions at 1940 and at 2073 and 2017 cm^{-1} which could be assigned to *trans*-$[Mn(CN)(CO)(dppm)_2]^+$ [15] and *cis*-$[RuCl(CO)_2(PPh_3)(o\text{-}O_2C_6Cl_4)]$ [11] respectively. As in **5**–**7** double oxidation appears to result in N–Ru bond cleavage. However further studies designed to isolate more robust doubly oxidised species are in progress in order to study the possibility of spin pairing between the paramagnetic manganese(II) and semiquinone centres.

Conclusions

(*i*) Cyanomanganese complexes can be used as ligands in the synthesis of redox-active heterobinuclear species such as *cis*-$[(dppe)(Et_3P)(OC)_2Mn(\mu\text{-}CN)Ru(CO)_2(PPh_3)(o\text{-}O_2C_6Cl_4)]$ and *trans*-$[(dppm)_2(OC)Mn(\mu\text{-}CN)Ru(CO)_2(PPh_3)(o\text{-}O_2C_6Cl_4)]$; the site of electron transfer can be systematically altered by modifying the ancillary ligands on manganese.

(*ii*) The unpaired electrons of the singly oxidised complexes *cis*- and *trans*-$[(dppm)\{(PhO)_3P\}(OC)_2Mn(\mu\text{-}CN)Ru(CO)_2(PPh_3)(o\text{-}O_2C_6Cl_4)]^+$ and *cis*-$[(dppe)(Et_3P)(OC)_2Mn(\mu\text{-}CN)Ru(CO)_2(PPh_3)(o\text{-}O_2C_6Cl_4)]^+$ are localised on the ruthenium-bound semiquinone ligand. Nevertheless, the formation of these complexes directly from *cis*- or *trans*-$[Mn(CN)(CO)_2\{P(OPh)_3\}(dppm)]$ or *cis*-$[Mn(CN)(CO)_2(PEt_3)(dppe)]$ and $[\{Ru(CO)_2(PPh_3)(\mu\text{-}o\text{-}O_2C_6Cl_4)\}_2]$ provides evidence for intramolecular electron transport through the cyanide bridge.

(*iii*) On oxidation, the shift in energy of ν(CN) indicates the site of oxidation in the heterobinuclear species; C-bonded site oxidation is accompanied by an increase in energy and N-bonded site oxidation by a decrease. The origin of this difference is as yet unknown but may have important diagnostic value. For example, isomerisation of the CN bridge [*e.g.* Mn(μ-CN)M to Mn(μ-NC)M] may be detectable (though such an isomerisation process has not yet been observed in our studies).

Experimental

The preparation, purification and reactions of the complexes described were carried out under an atmosphere of dry nitrogen, using dried, distilled, deoxygenated solvents. Unless stated otherwise (*i*) the complexes were purified by dissolving in CH_2Cl_2, filtering, adding hexane and reducing the solvent volume *in vacuo* to induce precipitation, and (*ii*) the complexes are air-stable solids which dissolve in polar solvents such as CH_2Cl_2 or thf to give moderately air-sensitive solutions. All of the reactions were carried out in flasks shielded from light by aluminium foil; where necessary the progress of a reaction was monitored by IR spectroscopy.

The compounds $[\{Ru(CO)_2(PPh_3)(\mu\text{-}o\text{-}O_2C_6Cl_4)\}_2]$,[11] *cis*- and *trans*-$[Mn(CN)(CO)_2\{P(OPh)_3\}(dppm)]$[3], *cis*-$[Mn(CN)(CO)_2(PEt_3)(dppe)]$,[5] *trans*-$[Mn(CN)(CO)_2L(L\text{–}L)][PF_6]$ [L = $P(OPh)_3$, L–L = dppm; L = PEt_3, L–L = dppe],[2] *trans*-$[Mn(CO)(NCMe)(dppm)_2][PF_6]$[15] and $[N_2C_6H_4F\text{-}p][PF_6]$[16] were prepared by published methods. The salt $[NO][PF_6]$ was purchased from Fluorochem Ltd., Glossop.

Electrochemical studies were carried out as previously described.[5] Under the conditions used, E° for the couples $[Fe(\eta\text{-}C_5H_5)_2]^+$–$[Fe(\eta\text{-}C_5H_5)_2]$ and $[Fe(\eta\text{-}C_5Me_5)_2]^+$–$[Fe(\eta\text{-}C_5Me_5)_2]$, used as internal standards, are 0.47 and −0.09 V respectively. Infrared spectra were recorded on a Nicolet 5ZDX FT spectrometer, and X-band ESR spectra on a Varian Associates 4502/15 spectrometer and calibrated against a solid sample of the diphenylpicrylhydrazyl (dpph) radical. Microanalyses were carried out by the staff of the Microanalytical Service of the School of Chemistry, University of Bristol.

trans-Bis[*bis(diphenylphosphino)methane*]*carbonylcyanomanganese*, *trans*-$[Mn(CN)(CO)(dppm)_2]$.—A mixture of $[Mn(NCMe)(CO)(dppm)_2][PF_6]$ (0.42 g, 0.41 mmol) and powdered $[NEt_4][CN]$ (0.19 g, 1.21 mmol) in toluene (50 cm^3) was heated under reflux for 25 min. Filtration of the warm solution, to remove a green precipitate, concentration of the filtrate to *ca.* 5 cm^3 *in vacuo*, and addition of hexane (60 cm^3) gave an orange precipitate which was washed with hexane and dried, yield 0.15 g (41%).

trans-Bis[*bis(diphenylphosphino)methane*]*carbonylcyanomanganese Hexafluorophosphate–Dichloromethane* (1/1), *trans*-$[Mn(CN)(CO)(dppm)_2][PF_6]\cdot CH_2Cl_2$.—To *trans*-$[Mn(CN)(CO)(dppm)_2]$ (47 mg, 0.054 mmol) in CH_2Cl_2 (10 cm^3) was added $[N_2C_6H_4F\text{-}p][PF_6]$ (13 mg, 0.050 mmol). After stirring for 5 min the red solution was filtered; addition of hexane (30 cm^3) gave a red precipitate which was purified from CH_2Cl_2–hexane, yield 22 mg (40%) (Found: C, 57.8; H, 4.2; N, 1.2. $C_{52}H_{44}F_6MnNOP\cdot CH_2Cl_2$ requires C, 57.5; H, 4.2; N, 1.3%). IR (CH_2Cl_2): ν(CO) 1938s; ν(CN) 2104w cm^{-1}. The complex is soluble in polar solvents such as CH_2Cl_2, thf and acetone to give red solutions which slowly decompose under nitrogen.

cis-$[(dppm)\{(PhO)_3P\}(OC)_2Mn(\mu\text{-}CN)Ru(CO)_2(PPh_3)(o\text{-}O_2C_6Cl_4)]$.—To a stirred solution of *cis*-$[Mn(CN)(CO)_2\{P(OPh)_3\}(dppm)]$ (50 mg, 0.06 mmol) in CH_2Cl_2 (20 cm^3) was added $[\{Ru(CO)_2(PPh_3)(\mu\text{-}o\text{-}O_2C_6Cl_4)\}_2]$ (40 mg, 0.03 mmol). After 5 min the bright orange solution was filtered and hexane (30 cm^3) added to precipitate the product. Purification from CH_2Cl_2–hexane gave orange microcrystals, yield 50 mg (56%). The complexes *cis*-$[(dppe)(Et_3P)(OC)_2Mn(\mu\text{-}CN)Ru(CO)_2(PPh_3)(o\text{-}O_2C_6Cl_4)]$ (67%), *trans*-$[(dppm)\{(PhO)_3P\}(OC)_2Mn(\mu\text{-}CN)Ru(CO)_2(PPh_3)(o\text{-}O_2C_6Cl_4)]$ (75%) and *trans*-$[(dppm)_2(OC)Mn(\mu\text{-}CN)Ru(CO)_2(PPh_3)(o\text{-}O_2C_6Cl_4)]$ (40%) were prepared similarly.

trans-$[(dppm)\{(PhO)_3P\}(OC)_2Mn(\mu\text{-}CN)Ru(CO)_2(PPh_3)(o\text{-}O_2C_6Cl_4)][PF_6]$.—To *trans*-$[Mn(CN)(CO)_2\{P(OPh)_3\}(dppm)][PF_6]$ (47 mg, 0.048 mmol) in CH_2Cl_2 (20 cm^3) was added $[\{Ru(CO)_2(PPh_3)(\mu\text{-}o\text{-}O_2C_6Cl_4\}_2]$ (32 mg, 0.024 mmol). After 45 min the red-brown solution was filtered, concentrated to *ca.* 5 cm^3 *in vacuo*, and treated with hexane (20 cm^3) to give an oily solid. Trituration of the oil with diethyl ether gave a solid which was purified by dissolution in a small volume of CH_2Cl_2, filtration and precipitation with diethyl ether as a red-brown solid, yield 24 mg (30%).

The complexes *cis*-$[(dppe)(Et_3P)(OC)_2Mn(\mu\text{-}CN)Ru(CO)_2(PPh_3)(o\text{-}O_2C_6Cl_4)][PF_6]$ (52%) and *trans*-$[(dppm)_2(OC)Mn(\mu\text{-}CN)Ru(CO)_2(PPh_3)(o\text{-}O_2C_6Cl_4)][PF_6]$ (43%) were prepared similarly; trituration was not always necessary. All of the salts are soluble in polar solvents such as CH_2Cl_2 and acetone to give solutions which only slowly decompose under nitrogen. The solids may be stored under nitrogen for prolonged periods.

Table 4 Atomic coordinates (× 10^4)

Atom	*x*	*y*	*z*
Ru	2 314(1)	5 680(1)	5 912(1)
Mn	1 273(1)	8 672(1)	6 803(1)
P(1)	3 045(1)	4 509(1)	5 582(1)
P(3)	1 990(1)	8 332(1)	7 632(1)
P(2)	2 213(1)	9 628(1)	6 585(1)
P(4)	385(1)	7 665(1)	7 024(1)
Cl(1)	2 619(1)	8 279(2)	4 635(1)
Cl(2)	4 177(2)	9 403(2)	4 960(1)
Cl(3)	5 313(1)	8 861(2)	5 998(1)
Cl(4)	4 821(1)	7 273(2)	6 717(1)
O(1)	2 398(2)	6 745(3)	5 374(1)
O(2)	3 337(2)	6 339(3)	6 278(2)
O(7)	218(3)	9 068(4)	5 810(2)
O(8)	678(3)	10 455(4)	7 228(2)
O(9)	2 213(3)	4 242(4)	6 746(2)
O(10)	796(3)	4 973(4)	5 285(2)
C(1)	3 031(3)	7 273(5)	5 515(2)
C(2)	3 240(4)	8 015(5)	5 205(2)
C(3)	3 935(5)	8 513(6)	5 358(3)
C(4)	4 426(4)	8 280(6)	5 815(3)
C(5)	4 223(4)	7 575(6)	6 136(3)
C(6)	3 524(4)	7 062(5)	5 990(3)
C(7)	634(4)	8 916(5)	6 198(3)
C(8)	925(4)	9 760(5)	7 066(2)
C(9)	2 258(4)	4 779(5)	6 429(3)
C(10)	1 365(3)	5 220(5)	5 526(2)
C(20)	3 602(4)	5 185(5)	5 221(3)
C(21)	4 341(4)	5 495(5)	5 450(3)
C(22)	4 726(5)	6 110(7)	5 187(4)
C(23)	4 389(6)	6 395(7)	4 702(4)
C(24)	3 664(6)	6 087(6)	4 475(3)
C(25)	3 261(4)	5 505(5)	4 734(3)
C(30)	2 529(4)	9 367(5)	8 000(2)
C(31)	2 155(4)	10 164(5)	8 184(2)
C(32)	2 553(5)	10 984(6)	8 424(3)
C(33)	3 337(5)	11 040(6)	8 495(3)
C(34)	3 709(4)	10 262(6)	8 331(3)
C(35)	3 312(4)	9 428(5)	8 090(2)
C(40)	2 661(4)	7 269(5)	7 808(2)
C(41)	2 977(4)	6 795(5)	7 457(2)
C(42)	3 507(4)	6 034(5)	7 594(3)
C(43)	3 731(4)	5 748(6)	8 085(3)
C(44)	3 430(4)	6 187(6)	8 444(3)
C(45)	2 906(4)	6 951(5)	8 305(3)
C(50)	−531(4)	8 261(5)	7 021(2)
C(51)	−796(4)	9 125(5)	6 742(2)
C(52)	−1 496(4)	9 544(5)	6 737(3)
C(53)	−1 939(4)	9 093(5)	7 009(3)
C(54)	−1 713(4)	8 229(6)	7 271(3)
C(55)	−1 010(4)	7 817(6)	7 284(3)
C(60)	73(4)	6 493(5)	6 671(2)
C(61)	−537(4)	6 528(6)	6 260(3)
C(62)	−787(5)	5 674(6)	5 972(3)
C(63)	−431(5)	4 766(6)	6 099(3)
C(64)	174(5)	4 718(6)	6 504(3)
C(65)	425(4)	5 575(5)	6 797(3)
C(70)	1 273(4)	8 031(5)	7 979(2)
C(71)	753(4)	7 216(5)	7 680(2)
C(80)	2 102(4)	9 671(5)	5 899(2)
C(81)	2 701(5)	10 240(6)	5 714(3)
C(82)	2 269(4)	10 980(5)	6 779(3)
C(83)	1 592(5)	11 590(6)	6 464(3)
C(84)	3 185(4)	9 153(5)	6 814(3)
C(85)	3 865(4)	9 875(7)	6 898(3)
C(90)	3 739(3)	3 801(5)	6 066(2)
C(91)	4 030(4)	4 206(6)	6 544(3)
C(92)	4 544(5)	3 687(8)	6 903(3)
C(93)	4 794(5)	2 760(7)	6 803(4)
C(94)	4 528(4)	2 327(6)	6 335(4)
C(95)	3 995(4)	2 845(5)	5 970(3)
C(110)	2 576(4)	3 493(5)	5 161(2)
C(111)	2 887(4)	3 118(6)	4 777(3)
C(112)	2 562(5)	2 270(6)	4 503(3)
C(113)	1 943(5)	1 809(6)	4 595(3)
C(114)	1 634(4)	2 156(5)	4 965(3)
C(115)	1 950(4)	3 001(5)	5 257(3)
C(100)	1 635(3)	7 506(4)	6 470(2)
N(100)	1 823(3)	6 856(4)	6 240(2)
C(200)	724(6)	8 364(13)	4 692(4)
Cl(20)	649(2)	8 389(3)	4 050(1)
Cl(30)	149(2)	7 302(3)	4 790(2)

cis-[(dppm){$(PhO)_3P$}$(OC)_2Mn(\mu\text{-}CN)Ru(CO)_2(PPh_3)$(*o*-$O_2C_6Cl_4$)][$PF_6$].—To a stirred solution of *cis*-[$(dppm)_2$-$(OC)Mn(\mu\text{-}CN)Ru(CO)_2(PPh_3)$(*o*-$O_2C_6Cl_4$)] (70 mg, 0.05 mmol) in CH_2Cl_2 (20 cm^3) was added [NO][PF_6] (8 mg, 0.05 mmol). After 30 min the dark red solution was filtered and hexane was added to give an oily red solid. Purification from CH_2Cl_2–hexane and washing with diethyl ether gave the product as a dark red solid, yield 50 mg (66%). The complex *cis*-[(dppe)$(Et_3P)(OC)_2Mn(\mu\text{-}CN)Ru(CO)_2(PPh_3)$(*o*-$O_2C_6$-$Cl_4$)]-[$PF_6$] (47%) was prepared similarly.

Crystal Structure Analysis of **7**·CH_2Cl_2.—*Crystal data*. $C_{62}H_{56}Cl_6MnNO_6P_4Ru$, $M = 1403.8$, monoclinic, space group $P2_1/c$, $a = 18.233(4)$, $b = 13.164(2)$, $c = 27.422(5)$ Å, $\beta = 104.69(2)°$, $U = 6366(2)$ Å^3, $Z = 4$, $D_c = 1.46$ g cm^{-3}, $\lambda = 0.710\,69$ Å, $\mu = 8.2$ cm^{-1}, $F(000) = 2856$, $T = 295$ K.

Diffraction measurements were made with a Nicolet four-circle P3m diffractometer using graphite-monochromated X-radiation on a single crystal mounted in a thin-walled glass capillary under N_2. Cell dimensions were determined from the setting-angle values of 14 centred reflections. A total of 9023 diffracted intensities (including checks) were measured in a unique quadrant of reciprocal space for $4.0 < 2\theta < 50.0°$ by ω–2θ scans of width $2.0° + \Delta\alpha_1\alpha_2$. Three check reflections (280, 2514, $\bar{4}00$) remeasured after every 50 ordinary data showed no crystal decay but an appropriate correction was applied for *ca.* 2% variation over the period of data collection. Of the non-check intensity data collected, 7703 unique observations remained after averaging of duplicate and equivalent measurements and deletion of systematic absences. Of these, 5977 with $I > 1.5\sigma(I)$ were retained for use in structure solution and refinement. An absorption correction was applied on the basis of 400 azimuthal scan data; maximum and minimum transmission coefficients were 0.957 and 0.825 respectively. Lorentz and polarisation corrections were applied. The structure was solved by heavy-atom (Patterson and Fourier difference) methods, and refined by blocked-cascade least squares against *F*. All non-hydrogen atoms were assigned anisotropic displacement parameters. All hydrogen atoms were constrained to ideal geometries with C–H 0.96 Å; aromatic hydrogens were assigned fixed isotropic displacement parameters (*ca.* 1.2 times that of the attached carbon), and methyl and ethyl hydrogens a common, refined, isotropic displacement parameter. Refinement of the 730 least-squares variables converged smoothly to residual indices $R = 0.054$, $R' = 0.050$, $S = 1.37$.* Weights, *w*, were set equal to $[\sigma_c^2(F_o) + gF_o^2]^{-1}$. Here $\sigma_c^2(F_o)$ is the variance in F_o due to counting statistics, and $g = 0.0005$ was chosen to minimise the variation in *S* as a function of F_o. Final difference electron-density maps showed no features outside the range +0.75 to −0.75 e Å^{-3}. Table 4 reports the positional parameters for the non-hydrogen atoms.

All calculations were made with programs of the

---

* $R = \Sigma|\Delta|/\Sigma|F_o|$; $R' = [\Sigma w\Delta^2/\Sigma wF_o^2]^{\frac{1}{2}}$; $S = [\Sigma w\Delta^2/(N_o - N_v)]^{\frac{1}{2}}$; $\Delta = F_o - F_c$ and N_o, N_v are the numbers of observations and variables.

SHELXTL[17] system as implemented on a Nicolet R3m/E structure determination system. Complex neutral-atom scattering factors were taken from ref. 18.

Additional material available from the Cambridge Crystallographic Data Centre comprises H-atom coordinates, thermal parameters and remaining bond lengths and angles.

Acknowledgements

We thank the SERC for a research studentship (to A. C. L.) and a post-doctoral research assistantship (to G. H. W.), Johnson Matthey plc for a generous loan of ruthenium salts, and Dr. D. A. V. Morton for assistance with the X-ray structure analysis.

References

1 Part 32, R. P. Aggarwal, N. G. Connelly, B. J. Dunne, M. Gilbert and A. G. Orpen, *J. Chem. Soc., Dalton Trans.*, 1991, 1.
2 N. G. Connelly, K. A. Hassard, B. J. Dunne, A. G. Orpen, S. J. Raven, G. A. Carriedo and V. Riera, *J. Chem. Soc., Dalton Trans.*, 1988, 1623.
3 G. A. Carriedo, M. C. Crespo, V. Riera, M. G. Sanchez, M. L. Valin, D. Moreiras and X. Solans, *J. Organomet. Chem.*, 1986, **302**, 47.
4 N. G. Connelly, A. G. Orpen, G. Rosair and G. H. Worth, unpublished work.
5 G. A. Carriedo, N. G. Connelly, M. C. Crespo, I. C. Quarmby and V. Riera, *J. Chem. Soc., Chem. Commun.*, 1987, 1806; G. A. Carriedo, N. G. Connelly, M. C. Crespo, I. C. Quarmby, V. Riera, and G. H. Worth *J. Chem. Soc., Dalton Trans.*, 1991, 315.
6 A. Christofides, N. G. Connelly, H. J. Lawson and A. C. Loyns, *J. Chem. Soc., Chem. Commun.*, 1990, 597.
7 See, for example, P. Rigo and A. Turco, *Coord. Chem. Rev.*, 1974, **13**, 167; P. L. Gaus and A. L. Crumbliss, *Inorg. Chem.*, 1976, **15**, 2080; J. A. Abys, G. Ogar and W. M. Risen, jun., *Inorg. Chem.*, 1981, **20**, 4446; A. J. Deeming, G. P. Proud, H. M. Dawes and M. B. Hursthouse, *J. Chem. Soc., Dalton Trans.*, 1988, 2475.
8 G. J. Baird, S. G. Davies, S. D. Moon, S. J. Simpson and R. H. Jones, *J. Chem. Soc., Dalton Trans.*, 1985, 1479.
9 B. I. Swanson, *Inorg. Chem.*, 1976, **15**, 253.
10 M. J. Freeman, Ph.D. Thesis, University of Bristol, 1984.
11 N. G. Connelly, I. Manners, J. R. C. Protheroe and M. W. Whiteley, *J. Chem. Soc., Dalton Trans.*, 1984, 2713.
12 L. P. Michiels, G. Kolks, E. R. Nesbitt, P. T. Dimauro, R. M. Kirchner and J. V. Waszczak, *Inorg. Chim. Acta*, 1985, **100**, 211.
13 See, for example, A. Bell, S. J. Lippard, M. Roberts and R. A. Walton, *Organometallics*, 1983, **2**, 1562; F. Scandola, C. A. Bignozzi, C. Chiorboli, M. T. Indelli and M. A. Rampi, *Coord. Chem. Rev.*, 1990, **97**, 299 and refs. therein.
14 R. E. Hester and E. M. Nour, *J. Chem. Soc., Dalton Trans.*, 1981, 939.
15 G. A. Carriedo, V. Riera, N. G. Connelly and S. J. Raven, *J. Chem. Soc., Dalton Trans.*, 1987, 1769.
16 A. Roe, *Org. React.*, 1949, **5**, 193.
17 G. M. Sheldrick, SHELXTL-PLUS, Revision 2.4, Göttingen, 1988.
18 *International Tables for X-Ray Crystallography*, Kynoch Press, Birmingham, 1974, vol. 4.

Received 15th *November* 1990; *Paper* 0/05142J